JOURNAL OF GEOPHYSICAL RESEARCH, VOL. 102, NO. B7, PAGES 15,489–15,505, JULY 10, 1997

The Southeast Indian Ridge between 88°E and 118°E: Variations in crustal accretion at constant spreading rate

Jean-Christophe Sempéré[1,2]

School of Oceanography, University of Washington, Seattle

James R. Cochran

Lamont-Doherty Earth Observatory of Columbia University, Palisades, New York

SEIR Scientific Team[3]

Abstract. The temperature of the mantle and the rate of melt production are parameters which play important roles in controlling the style of crustal accretion along mid-ocean ridges. To investigate the variability in crustal accretion that develops in response to variations in mantle temperature, we have conducted a geophysical investigation of the Southeast Indian Ridge (SEIR) between the Amsterdam hotspot and the Australian-Antarctic Discordance (88°E- 118°E). The spreading center deepens by 2100 m from west to east within the study area. Despite a uniform, intermediate spreading rate (69-75 mm yr^{-1}), the SEIR exhibits the range in axial morphology displayed by the East Pacific Rise and the Mid-Atlantic Ridge (MAR) and usually associated with variations in spreading rate. The spreading center is characterized by an axial high west of 102°45'E, whereas an axial valley is prevalent east of this longitude. Both the deepening of the ridge axis and the general evolution of axial morphology from an axial high to a rift valley are not uniform. A region of intermediate morphology separates axial highs and MAR-like rift valleys. Local transitions in axial morphology occur in three areas along the ridge axis. The increase in axial depth toward the Australian-Antarctic Discordance may be explained by the thinning of the oceanic crust by ~4 km and the change in axial topography. The long-wavelength changes observed along the SEIR can be attributed to a gradient in mantle temperature between regions influenced by the Amsterdam and Kerguelen hot spots and the Australian-Antarctic Discordance. However, local processes, perhaps associated with an heterogeneous mantle or along-axis asthenospheric flow, may give rise to local transitions in axial topography and depth anomalies.

Introduction

Available geophysical and geochemical constraints on mid-ocean ridge processes have established that spreading rate is an important controlling parameter in crustal accretion [*Macdonald*, 1982]. Because it accounts for much of the global variability in mid-ocean ridges, spreading rate can be argued to be the most important crustal accretionary variable. The fastspreading East Pacific Rise and the slow spreading Mid-Atlantic Ridge illustrate the range in the characteristics of mid-ocean ridges, such as axial morphology, gravity signature, chemical variability, and segment geometry, that can arise due to variations in spreading rate. The existence of large variations in physical and chemical observables at uniform spreading rate along some spreading centers indicates, however, that other parameters may also play an important role in dictating the style of accretion of oceanic lithosphere. Among these parameters, the temperature of the mantle and the rate of melt production relative to spreading rate have a particular importance as demonstrated, for instance, by the pronounced physico-chemical gradients observed near ridge-influenced hot spots and by the global correlation between axial depth and $Na_{8.0}$ [*Klein and Langmuir*, 1987].

The study of the different parameters that influence crustal accretion requires the identification of areas where such parameters vary while spreading rate remains constant. The Southeast Indian Ridge (SEIR) between Amsterdam and St. Paul Islands and the Australian-Antarctic Discordance (AAD) is one location along the mid-ocean ridge system amenable to such a study. This portion of the SEIR is located between a section of the spreading axis influenced by the Amsterdam and Kerguelen hot spots and a region of cold, and potentially downwelling, mantle beneath the AAD. Located close to the equator of the pole of rotation of the Indo-Australian and Antarctic plates [*DeMets et al.*, 1990], this section of the SEIR exhibits small variations in spreading rate. Finally, the Southeast Indian

[1]Also at Groupe de Recherche en Géodésie Spatiale, UMR-5566, Observatoire Midi-Pyrénées, Toulouse, France.

[2]Now at Exxon Production Research Company, Houston, Texas.

[3]Southeast Indian Ridge (SEIR) Scientific Team (D. Christie, College of Oceanic and Atmospheric Sciences, Oregon State University; M. Eberele, Department of Geological Sciences, Brown University; L. Géli, Département de Géosciences Marines, IFREMER; J. A. Goff, University of Texas Institute of Geophysics; H. Kimura, Earthquake Research Institute , University of Tokyo; Y. Ma, Lamont-Doherty Earth Observatory of Columbia University; A. Shah, School of Oceanography, University of Washington; C. Small, Lamont-Doherty Earth Observatory of Columbia University; B. Sylvander, College of Oceanic and Atmospheric Sciences, Oregon State University; B.P. West, School of Oceanography, University of Washington; and W. Zhang, Lamont-Doherty Earth Observatory of Columbia University).

Paper number 97JB00171.
0148-0227/97/97JB-00171$09.00

Ridge is an intermediate spreading center and, as such, small perturbations in melt production may affect its geophysical characteristics drastically [*Chen and Morgan*, 1990a, b; *Phipps Morgan and Chen*, 1993].

Our knowledge of spreading centers in the Southern Ocean lags that of the Mid-Atlantic Ridge and East Pacific Rise. With the exception of isolated geophysical transects conducted in the 1960's and 1970's, our understanding of the Southeast Indian Ridge west of the AAD comes primarily from satellite altimetry. Satellite gravity data indicate that the characteristics of crustal accretion vary between Amsterdam Island and the AAD. *Small and Sandwell* [1989, 1992] have shown that a transition from a rough, high-amplitude gravity field to a smooth, low-amplitude field occurs along the SEIR near 100°E. This transition is likely due to a change in axial morphology from an axial high to a rift valley. Indeed, a rift valley is observed between 101°E and the AAD on all previously collected bathymetric profiles, whereas an axial high is generally observed on profiles between 82°E and 101°E [*Ma and Cochran*, 1996]. Because the morphology of the ridge axis is a function of its rheological and thermal structure and of the stresses applied to the plates, the existence of morphological transitions along the plate boundary at constant spreading rate suggests that the gradient in mantle temperature between Amsterdam Island and the AAD inferred from seismic studies [e.g., *Forsyth et al.*, 1987; *Yan et al.*, 1989; *Roult et al.*, 1994; *Su et al.*, 1994] constitutes an important perturbation to the "normal" accretionary regime.

We have conducted a detailed geophysical and geochemical study of the Southeast Indian Ridge between 88°E and 118°E (Figure 1) with the goal of obtaining observational constraints on the variations in style of crustal accretion at constant spreading rate in an area where a large gradient in mantle temperature is present. The west end of our survey area is located approximately 1300 and 2400 km from the Amsterdam and Kerguelen Islands, respectively, and the east end is about 400 km away from the center of the Australian-Antarctic Discordance. In this paper and in the companion paper by *Cochran et al.*, [this issue] we present the preliminary results of the geophysical and geochemical components of our study. Detailed analyses of the observations and processes discussed in the present paper will be addressed in future, in-depth studies (A. Shah and J.-C. Sempéré, The transition from axial high to rift valley morphology and the relation to variations in mantle temperature, submitted to *Journal of Geophysical Research*, 1997, hereinafter referred to as Shah and Sempéré, submitted manuscript, 1997; Y. Ma and J. R. Cochran, Bathymetric roughness of the Southeast Indian Ridge: Implications for crustal accretion at intermediate spreading rate mid-ocean ridges, submitted to *Journal of Geophysical Research*, 1997, hereinafter referred to as Ma and Cochran, submitted manuscript, 1997; B. P. West and J.-C. Sempéré, Gravity anomalies, flexure of axial lithosphere and along-axis mantle flow between 98°E and 112°E along the Southeast Indian Ridge, submitted to *Earth and Planetary Science Letters*, 1997, hereinafter referred to as West and Sempéré, submitted manuscript, 1997; C. Small et al., manuscript in preparation, 1997).

Data Acquisition

The data discussed in this paper were acquired during two recent field programs aboard the R/V *Melville* (Figure 1). The first leg, which took place between December 1994 and January 1995, consisted of a geophysical survey of the Southeast Indian Ridge between 91°E and 118°E. Although the second field program (February-March 1995) was primarily a sampling leg, additional geophysical coverage was obtained between 88°E and 91°E. A 2500-km-long section of the ridge axis was surveyed during the two field programs. This coverage includes four detailed study areas, encompassing eight second-order ridge segments, which extend out to 1.2 Myr lithosphere, for a total ridge length of 1100 km. Within each box, Sea Beam 2000 bathymetry, magnetics, and gravity lines perpendicular or slightly oblique to the axis, and extending out about 45 km on either side, were obtained with a 9-km spacing, providing almost full bathymetric coverage.

General Characteristics of the Southeast Indian Ridge

The Southeast Indian Ridge separates the Indo-Australian and the Antarctic plates. It extends from the Macquarie to the Rodrigues Triple Junction. Spreading rate along the SEIR, calculated using the NUVEL-1A pole [*DeMets et al.*, 1990], varies from 69 mm yr^{-1} near 88°E to 75 mm yr^{-1} near 120°E. Between 102°E and the east end of our study area, spreading rate is essentially constant. The morphology of the left-stepping transform faults in our survey area, which suggests a component of extension oblique to the offsets, and the presence of a long, elevated ridge, interpreted to be a compressional feature, within the transform domain of the right-stepping 96°E transform point to a recent counterclockwise change in the relative motion of the two plates [*Sempéré et al.*, 1995; C. Small et al., manuscript in preparation, 1997].

Segmentation Characteristics

The Southeast Indian Ridge between 88°E and 118°E includes nine transform faults located near 88°30'E, 96°E, 100°E, 102°45'E, 105°10'E, 106°30'E, 108°30'E, 114°30'E, and 116°E (Figures 2 and 3). Offsets along these transforms range from 21 to 135 km, corresponding to age offsets of 0.5 to 3.6 Ma. The two smallest offset transforms are located near 102°45'E and 108°30'E. Because it lacks an off-axis fracture zone extension observable in bathymetric data, the 102°45'E Transform must have been initiated in the last 1 Myr (Figure 4) [*Small et al.*, 1995; Shah and Sempéré, submitted manuscript, 1997]. The trace of the 108°30'E transform in satellite gravity data shows that it has not been stable with time and that it may be evolving into a nontransform offset (Figure 2) [*Small et al.*, 1995; Shah and Sempéré, submitted manuscript, 1997]. The SEIR between 88° and 118°E consists of eight first-order segments if only transform faults fixed with respect to the spreading axis for more than 5 Myr are counted as first-order discontinuities [*Small et al.*, 1995, also manuscript in preparation, 1997]. In addition to transform faults, we observe the presence of five actively propagating rifts migrating eastward. The transform faults and the propagating rifts are located at local maxima in axial depth (Figure 2).

Since the new bathymetric coverage only extends out to 1.2 Myr at its widest, we have used satellite gravity data (D.T. Sandwell and W.H.F. Smith, Marine gravity field from satellite altimetry, version 7.2, Geological Data Center, Scripps Institution of Oceanography, 1995 (available as digital file anonymous ftp to baltica.ucsd.edu) (hereinafter cited as digital

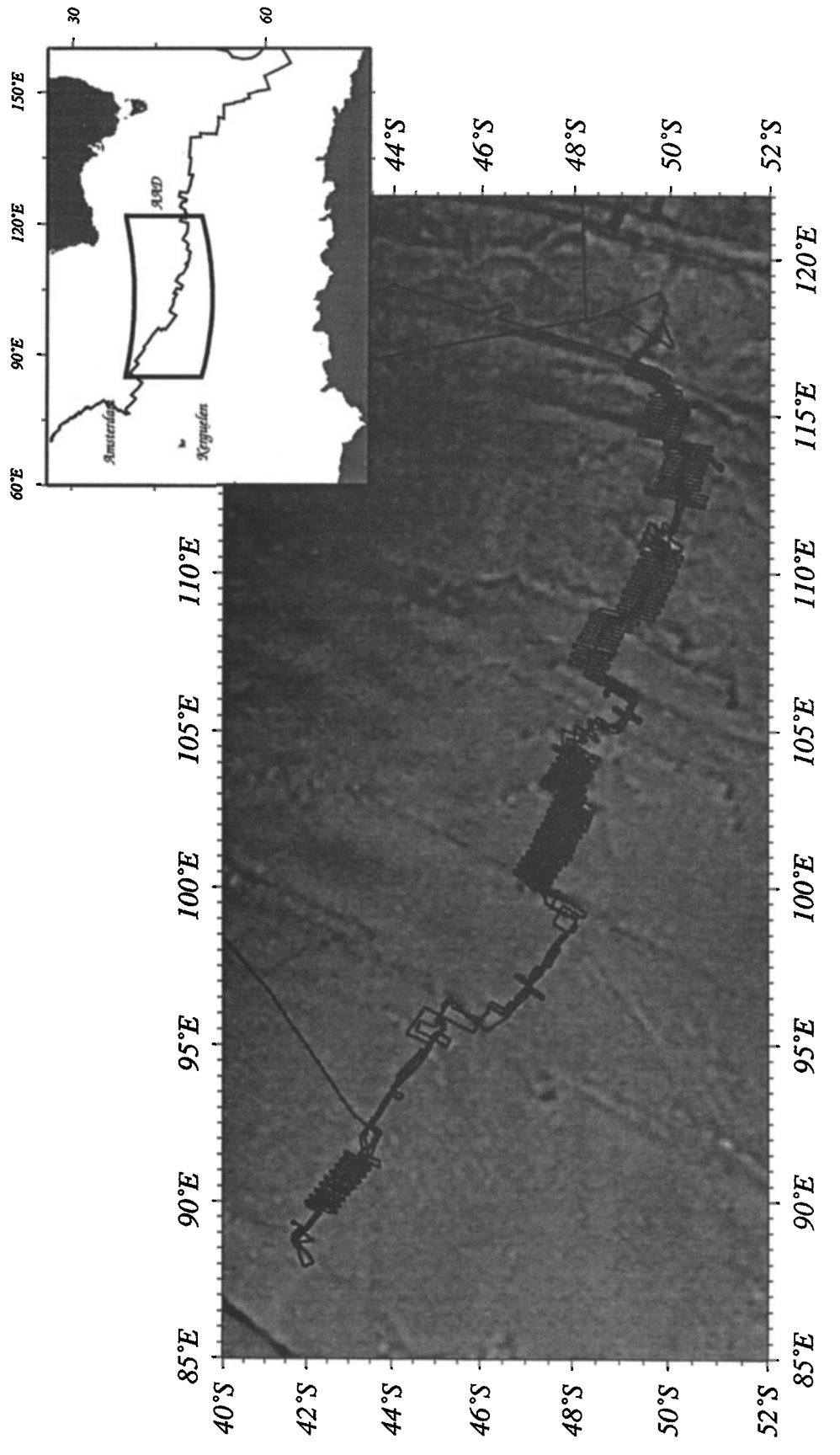

Figure 1. Track coverage obtained over the Southeast Indian Ridge during leg West09 and West10 of the R/V *Melville*. Ship tracks are superposed on satellite gravity data (Sandwell and Smith, digital file, 1995). Inset shows location of survey area.

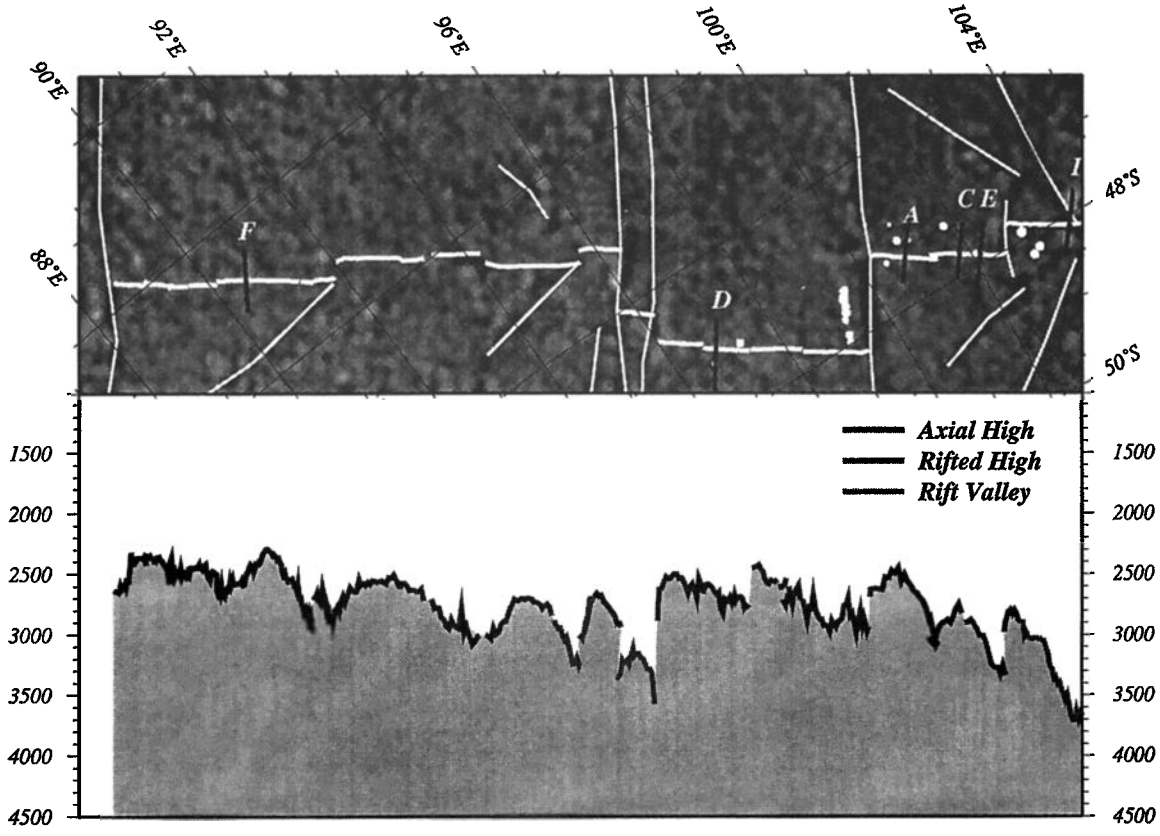

Figure 2a. (top) Geometry of the plate boundary (white lines) between 88°E and 104°10'E. Plate boundary is superposed on satellite gravity data [*Sandwell and Smith*, 1995]. Seamounts with diameters greater than 3 km mapped during survey are shown as white dots. Labeled, solid lines perpendicular to the ridge axis indicate the location of cross-axis profiles shown in Figure 6. (bottom) Axial depth along the plate boundary. The morphology of the spreading axis is coded by shading (see legend). Transform faults, propagating ridges, and second-order offsets are located at local depth maxima.

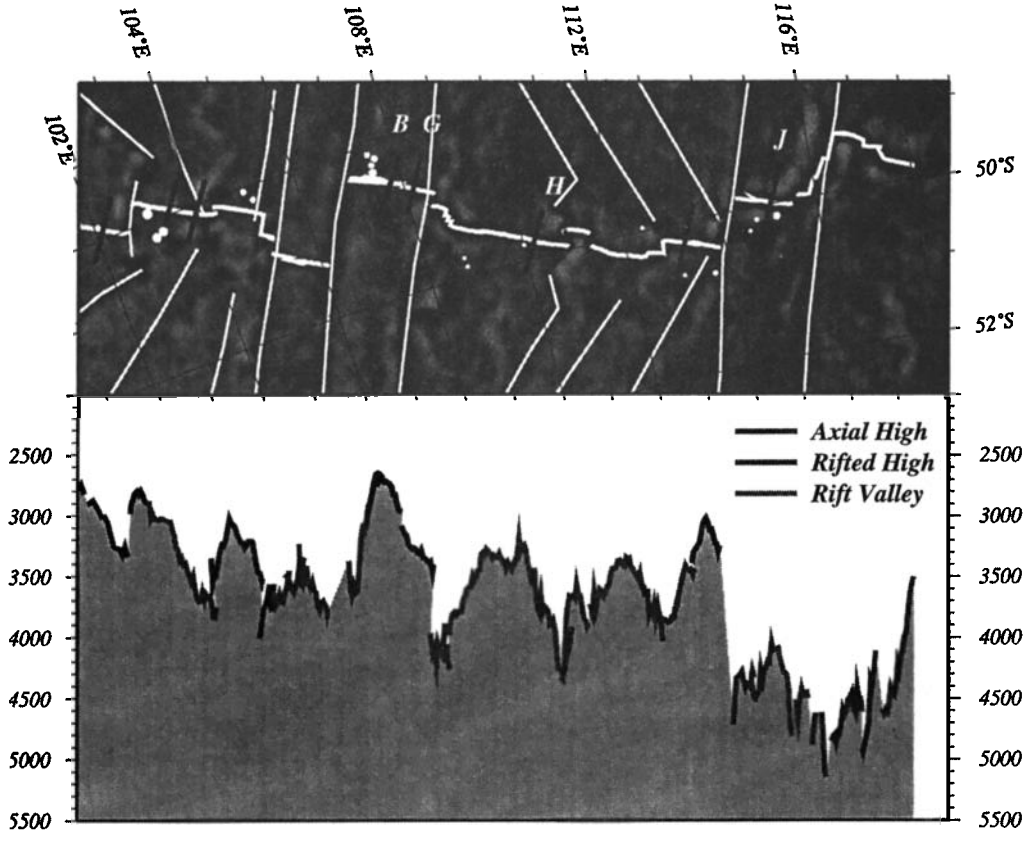

Figure 2b. (top) Geometry of the plate boundary between 101°30'E and 118°E. See Figure 2a for caption. (bottom) Axial depth along the plate boundary.

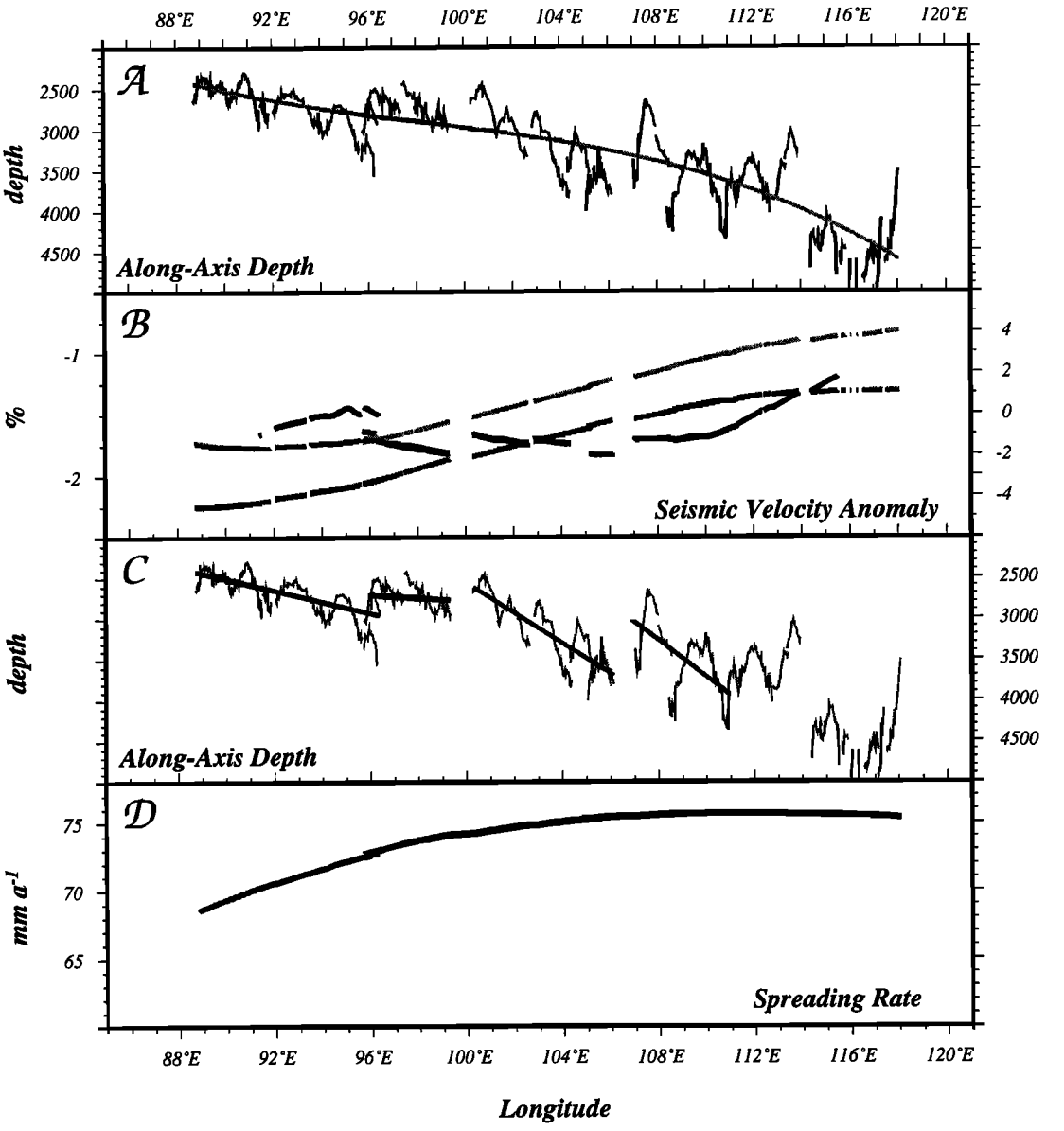

Figure 3. (a) Axial depth as a function of longitude. A third-order polynomial has been fit to the depth profile from 88°E to 120°E to mark the long-wavelength increase of the spreading axis from west to east. (b) Shear wave velocity anomaly at a depth of 150 km (dark gray line) and 250 km (light gray line, vertical axis is on the left) [*Su et al.*, 1994] and phase velocity anomaly for a period of 200 s (solid line, vertical axis is on the right) [*Roult et al.*, 1994] beneath the Southeast Indian Ridge. The long-wavelength decrease in axial depth is correlated with the increase in shear wave and phase velocity from west to east. (c) Uniform depth gradients at intermediate wavelength may characterize sections of the spreading center bounded by first-order discontinuities between 88°E and 111°E (see text). (d) Spreading rate along the plate boundary using the NUVEL-1A pole [*DeMets et al.*, 1990].

file) to obtain information regarding the evolution of the plate boundary. The structures which dominate the satellite gravity data on the flanks of the study area are fracture zones perpendicular to the axis and lineated gravity highs and lows oblique to the spreading direction (Figures 1 and 2). Some of these lineations form zig-zag structures alternatively pointing east and west. The off-axis perspective provided by satellite gravity data shows that segmentation along the SEIR has been and is being modified by both unidirectional and dual propagation through time. Thus the configuration of the plate boundary evolves rapidly within corridors bounded by the transforms that have been stable with time (C. Small et al., manuscript in preparation, 1997).

First-order segments are further partitioned by 19 nontransform discontinuities (NTD) with offsets varying from 2 to 17 km. These offsets bound second-order segments that have lengths varying from 18 to 180 km. Smaller offsets of the axis not associated with maxima in along-axis depth and with disrupted flank topography indicative of some degree of temporal stability are interpreted as minor expressions of volcanic partitioning and are not included in this study. Although significant scatter exists, the mean length of

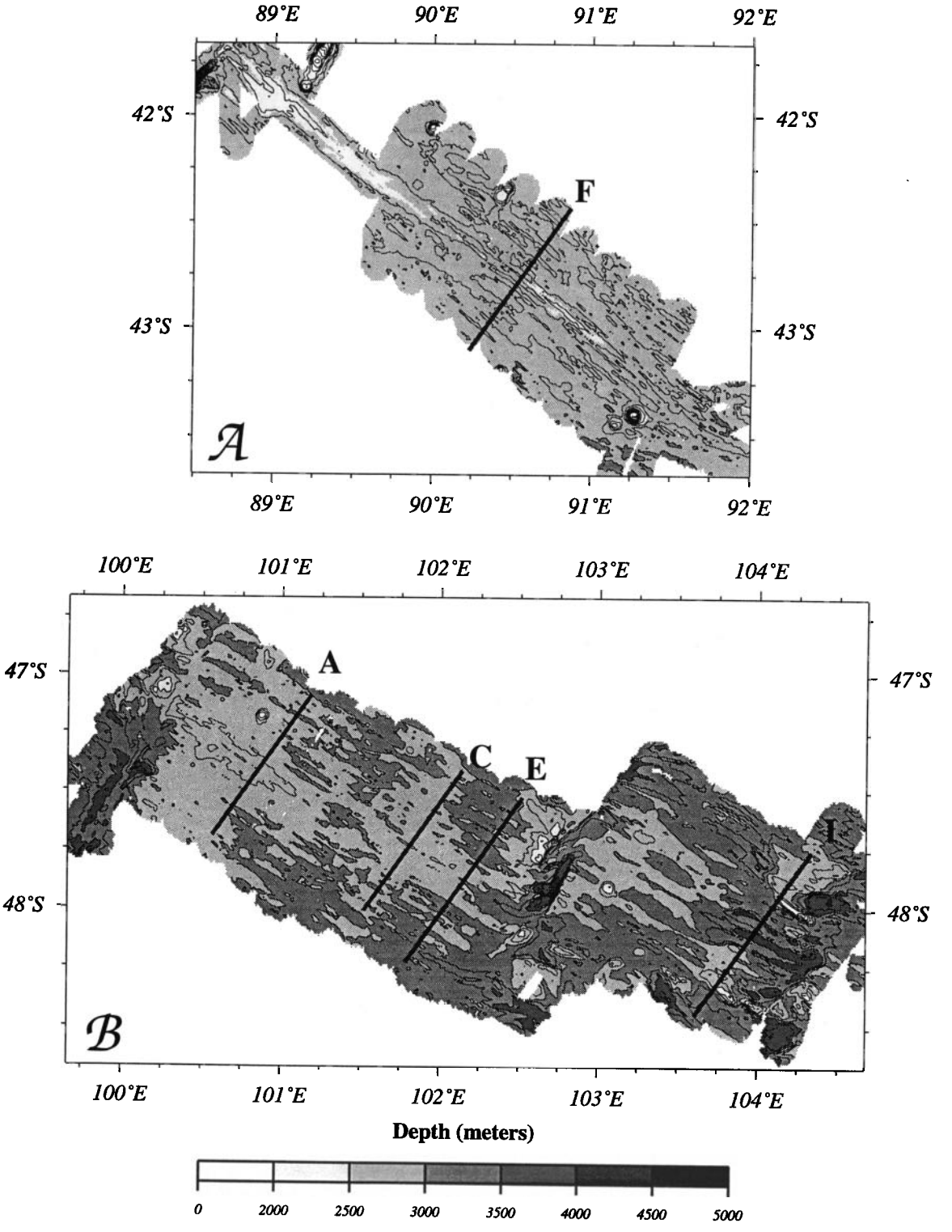

Figure 4. Bathymetry of the four areas surveyed out to 1.2 Myr old lithosphere on the flanks of the SEIR. Bold lines and labels refer to the bathymetric profiles shown in Figure 6. (a) The SEIR between 88°30'E and 92°00'E is characterized by an axial high cut by a narrow depression (contour interval is 200 m). (b) The morphology of the axis in the three segments of the SEIR between 100°E and 104°E evolves from an axial high to the west to a rift valley to the east (contour interval is 250 m). The easternmost discontinuity is the 104°20'E propagating rift. (c) Between 107°E and 111°30'E, the SEIR consists of two segments separated by a complex, short-offset transform (contour interval is 250 m). The axial high in the western segment is located on a plateau. The high evolves into a shallow valley east of 108°E. The eastern segment is characterized by a shallow axial valley. (d) East of 114°E, near the Australian-Antarctic Discordance, the spreading center is associated with a rift valley (contour interval is 500 m). The segment located between the 112°45'E propagating ridge and the 114°E transform exhibits a local transition in morphology from a shallow axial valley to the west to a low axial high to the east.

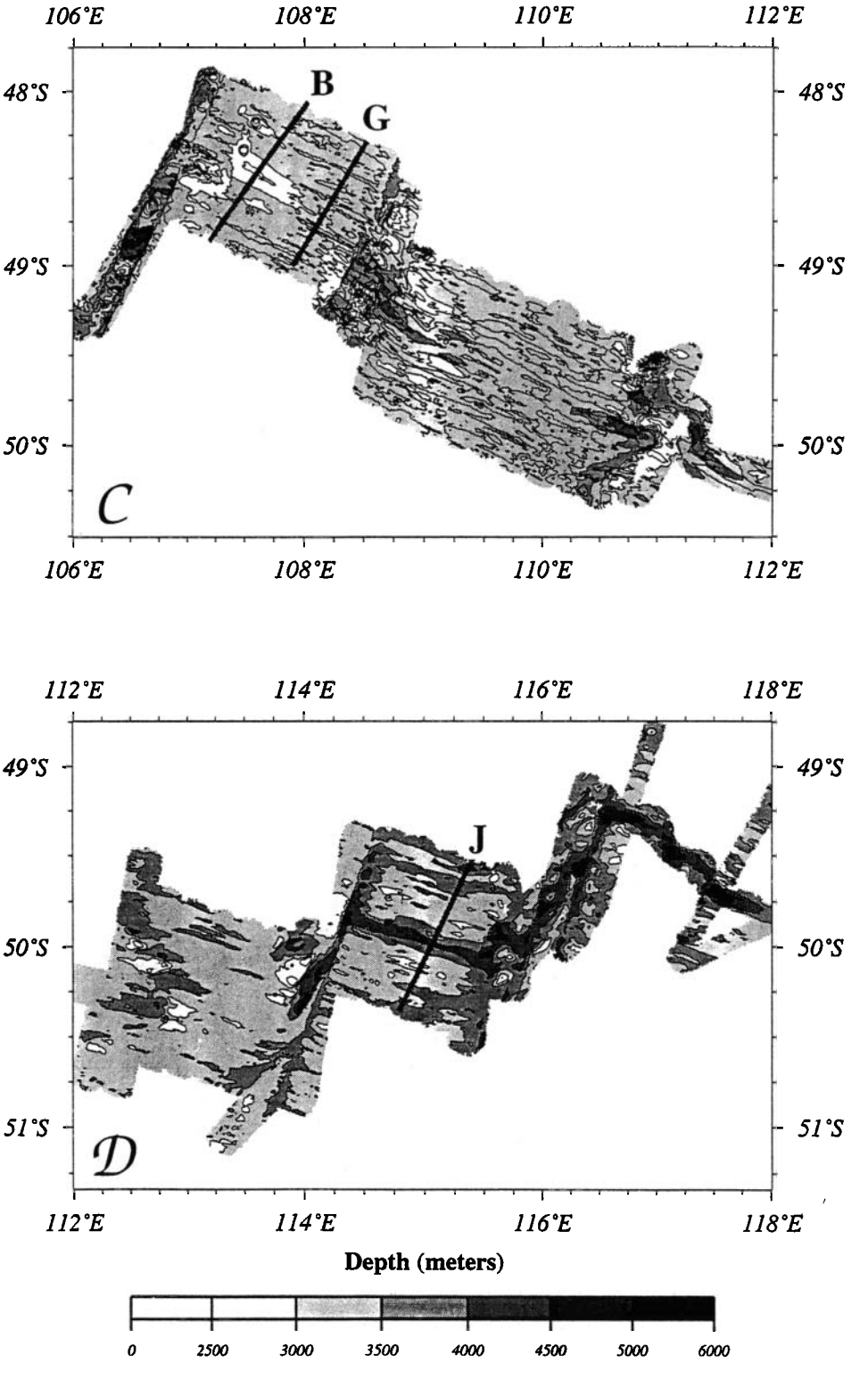

second-order segments diminishes from 80 km at the west end of our coverage to 60 km at the east end (Figure 5). This change in segment length is similar to that observed between the East Pacific Rise (EPR) near 9°N [*Macdonald et al.*, 1984] and the Mid-Atlantic Ridge (MAR) between 24° and 30°N [*Sempéré et al.*, 1993].

Along-Axis Depth Variations

The Southeast Indian Ridge increases in depth by over 2100 m from 88°E to 118°E (Figures 2 and 3). The minimum depth within each segment ranges from ~ 2300 m in the western most segment to ~ 4400 m near the east end of our survey. The

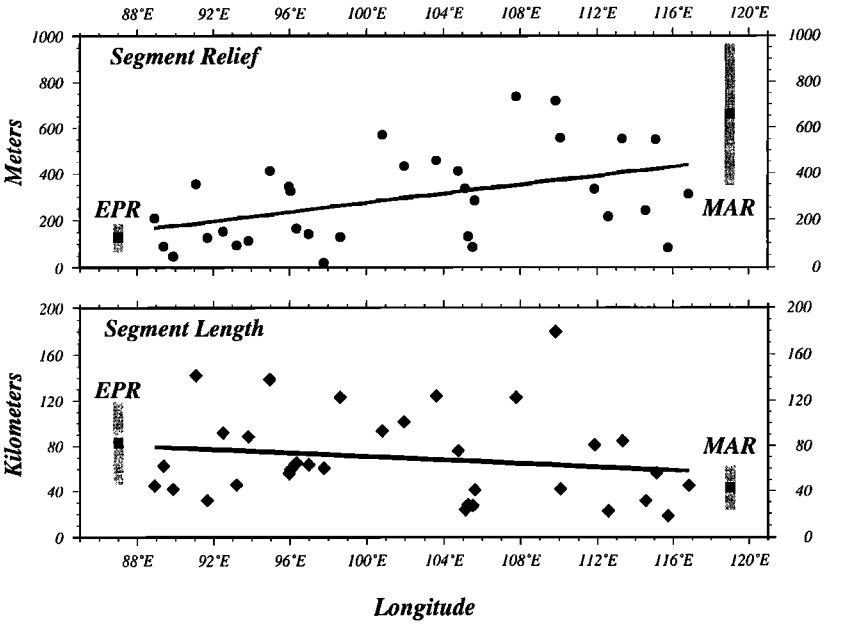

Figure 5. (top) Relief within second-order segments along the plate boundary. Segment relief is measured as the mean value of the difference in axial depth between the segment ends and the shallowest axial depth within the segment. The eastward increase in segment relief is interpreted as resulting from variations in crustal thickness in the eastern part of the survey area. The range in segment relief observed along the SEIR reproduces that observed between the Mid-Atlantic Ridge (MAR) between 24° and 30°N [*Sempéré et al.*, 1993] and the East Pacific Rise (EPR) between 10°N and 14°N [*Macdonald et al.*, 1984]. (bottom) Variation in the length of second-order segments along the plate boundary. The range in segment length observed along the SEIR reproduces that observed between the Mid-Atlantic Ridge (MAR) between 24° and 30°N [*Sempéré et al.*, 1993] and the East Pacific Rise (EPR) near 9°*N [Macdonald et al.*, 1984].

increase in depth from 88°E to 118°E defines a long-wavelength variation which is correlated with the increase in the shear wave and phase velocity anomalies obtained in tomographic models (Figure 3) [*Su et al.*, 1994; *Roult et al.*, 1994]. Superposed on the long-wavelength depth increase, we observe intermediate-wavelength (200-400 km) depth variations and short-wavelength (50-100 km) depth undulations.

Between 88°E and 111°E, we can decompose the axis of accretion into four regions in which the depth of the spreading center increases uniformly toward the east (Figure 3). Depth gradients within these corridors are 0.90, 0.30, 2.50, 3.05 m km^{-1} from west to east. These intermediate-wavelength depth variations are bounded by transform faults or propagating rifts, but all propagators do not modify significantly the along-axis depth gradient. East of 111°E, the close spacing of transforms and propagating rifts (Figure 2) precludes the development of intermediate wavelength depth gradients. The axial depth steps up abruptly (> 500 m) from west to east at the boundaries between intermediate-wavelength units. Thus the increase in the depth of the spreading center toward the AAD is not uniform (Figure 3).

At short wavelengths (50-100 km), depth maxima are located at the end of second-order segments, and depth minima are located near the middle of segments. The pattern of short-wavelength depth variations, and its association with second-order segments, is similar to that observed at fast and slow spreading centers [e.g., *Macdonald et al.*, 1984; *Sempéré et al.*, 1990]. The relief in axial depth along segments increases from 160 m at the west end of our coverage to 450 m at the east end (Figure 5). For comparison, the relief in axial depth within segments of the EPR between 10° and 14°N and along the MAR between 24° and 30°N are 129 ± 64 m [*Macdonald et al.*, 1984] and 658 ± 312 m [*Sempéré et al.*, 1993], respectively.

Axial Morphology

Three broad types of axial topography are encountered along the SEIR between 88° and 118°E: axial highs (profile A in Figure 6), rifted highs (profiles B-F in Figure 6), and axial valleys (profiles G-J in Figure 6). Axial highs refer to the axial morphology observed along most of the length of the (EPR) such as near 3°30'S [*Lonsdale*, 1977]. Axial valley morphology includes both shallow rift valleys (< 400 m; for instance between 112°45'E and 114°E) as well as deep rift valleys akin to those found along the Mid-Atlantic Ridge (MAR) such as near 37°N [*Macdonald*, 1982]. An EPR-like axial high is observed in but a few locations along the SEIR (Figure 2). Rifted highs are more common. In our nomenclature, rifted high morphology is characterized by the presence of a narrow depression, 50-200 m deep, at the summit of an axial high. Although the different morphologies encountered along the SEIR can be made to fit into the three broad categories listed above, such a classification is in fact too rigid to express the variability in morphology observed along the plate boundary. The rifted high and axial valley regions include flat axial topography and shallow axial valleys very distinct from MAR-like rift valleys that are seldom seen elsewhere (Figure 6). Such morphologies have been termed intermediate in the analysis of *Goff et al.* [1997].

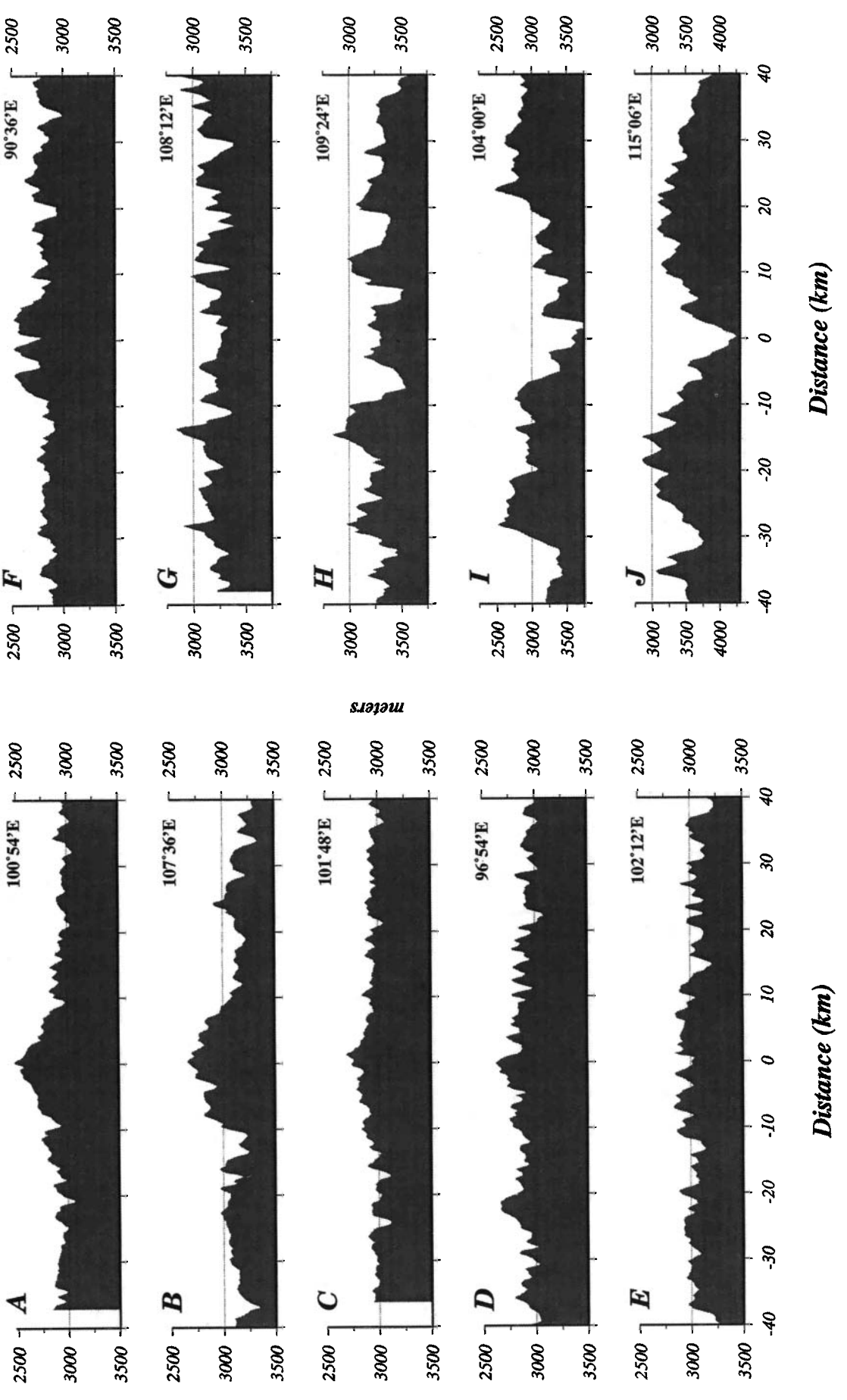

Figure 6. Cross-axis bathymetric profiles illustrating the range in axial morphology observed over the survey area. The different morphologies are ordered qualitatively from axial high to rift valley. The location of profiles is indicated on Figures 2 and 3. Note that the evolution from an axial high to the west to a rift valley to the east is not uniform. Examples of axial highs as shown on profiles A or B are rare. Profiles A, C, E, and I sample the transition in axial morphology observed between 100°E and 104°E (see Figure 4).

A detailed classification of the morphology of the SEIR is beyond the scope of this paper. For an in-depth analysis of axial morphology, the reader is referred to *Goff et al.* [1997], Shah and Sempéré (submitted manuscript, 1997) and Ma and Cochran (submitted manuscript, 1997).

The morphology of the spreading axis evolves from west to east (Figures 2 and 4). Axial highs and rifted highs dominate the morphology of the SEIR west of 102°45'E (Figure 2). Axial highs and rifted highs are also found along the SEIR east of the AAD [*Sempéré et al.*, 1996]. If a gradient in mantle temperature is ultimately responsible for the long-wavelength evolution of axial morphology, we would expect the morphology the most indicative of high melt production [e.g., *Scheirer and Macdonald*, 1993] to be observed at the west end of the survey. However, the clearest example of an axial high does not come from segments close to the west end of our coverage. Instead, our westernmost survey box exhibits an axial high cut by small-throw normal faults close to the axis (Figure 4a). An EPR-like crosssection is seen farther east near 101°E and 107°30'E (Figure 6, profile A). Shallow axial valleys dominate east of 108°30'E, and deep, MAR-like rift valleys are observed east of 114°E. Our easternmost survey box is characterized by a >1000-m-deep rift valley similar in its characteristics to that found along the MAR between the Kane and Atlantis Transforms [*Sempéré et al.*, 1993] or in the FAMOUS area [*Macdonald and Luyendyk*, 1977]. The same morphology is also found in the Australian-Antarctic Discordance farther east [*Palmer et al.*, 1993]. Thus the 102°45'E transform separates the SEIR into one section where axial highs dominate and a transitional region. This regional boundary coincides approximately with the transition between rough and smooth gravity profiles noted by *Small and Sandwell* [1989]. The boundary between the transitional region and the region characterized by deep rift valleys is found near 114°E.

The general evolution in axial morphology that we observe from 88°E to the Australian-Antarctic Discordance is also apparent in the characteristics of abyssal hills on the flanks of the spreading center. Statistical analysis of bathymetric data indicate that the rms height and characteristic width of abyssal hills increase from west to east, reflecting the evolution from axial high to intermediate morphology and finally to rift valley topography [*Goff et al.*, 1997]. Comparison of abyssal hill statistics along the SEIR with those along the MAR and EPR indicates that the full range of variability between the MAR and EPR is seen along the SEIR, and that this range is strongly correlated to axial morphology.

Nontransform Offsets

The morphology of nontransform discontinuities (NTD) also evolves along strike from west to east. Small offsets of the ridge axis are accommodated by overlapping spreading centers (OSC) or minor jogs in the neovolcanic zone at the crest of the ridge axis west of 101°25'E. East of 101°25'E, nontransform offsets consist mostly of intravalley jogs of the neovolcanic zone, some of which are associated with abrupt steps of the rift valley walls, such as are observed along the Mid-Atlantic Ridge (MAR) (Figure 7) [e.g., *Grindlay et al.*, 1991; *Sempéré et al.*, 1993]. Because the overlapping spreading centers (OSC) near 101°25'E is the easternmost offset before the 102°45'E transform, the transition from OSCs to MAR-like discontinuities can be taken as coinciding with the regional transition in axial morphology described in the preceding section. The morphology of OSCs along the SEIR varies with that of the limbs of the offset spreading axes from overlapping axial highs to overlapping rifted highs (Figure 7). Two of the OSCs located where off-axis coverage is available (90°35'E and 101°20'E) are associated with a trace, consisting of curved ridges and faults, oblique to the spreading direction indicating that the offset has propagated east.

Rift Propagation

There are five active propagating ridges along the Southeast Indian Ridge between 88°E and 118°E (Figures 2 and 8). They are located near 91°45'E, 95°40'E, 104°20'E, 111°00'E, and 112°45'E (Figure 8). The offset across the propagating rifts range from 16 to 29 km. Two additional propagating ridges have recently collided against the 114°E transform and 116°E transform. All of these offsets are or were propagating toward the east, like the two OSCs noted previously, down the slope of the long-wavelength bathymetry gradient. Adequate off-axis coverage is only available for determination of the propagation rate at 111°00'E (propagation rate is 31-37 mm yr^{-1}) and 112°45'E (53 mm yr^{-1}). The propagation rate of the 91°45'E (51 mm yr^{-1}), 95°40'E (45 mm yr^{-1}), and 104°20'E (44 mm yr^{-1}) propagators can be estimated from satellite gravity. These propagating ridges have left V-shaped traces in satellite gravity data on the flanks of the spreading center (Figures 1 and 2) [*Phipps Morgan and Sandwell*, 1994].

Based on bathymetric evidence and on satellite gravity data [this paper; *Phipps Morgan and Sandwell*, 1994; *Sempéré et al.*, 1996; C. Small et al., manuscript in preparation, 1997], ridge propagation has been the dominant mechanism in the recent evolution of the plate boundary between 88°E and 140°E. Shipboard bathymetry and satellite gravity data indicate that three propagating rifts are actively migrating west along the Southeast Indian Ridge east of the AAD [*Phipps Morgan and Sandwell*, 1994; *Sempéré et al.*, 1996]. Satellite gravity and aeromagnetic data indicate that rift propagation has occurred repeatedly in the past [*Phipps Morgan and Sandwell*, 1994; *Vogt et al.*, 1984]. The collision of a propagating rift with a transform may result in the reorientation of the direction of slip between two offset limbs of a spreading center. Such a change in slip direction has occurred at the 114°E transform (Figure 4b).

Transitions in Axial Morphology

The long-wavelength depth increase of the spreading center corresponds to a general evolution in axial morphology from an axial high to a rift valley from west to east. However, the change in morphology, like the increase in the depth of the axis, is not uniform (Figure 2). There are three local morphological transitions between 88° and 118°E: 100-104°, 106-111°, and near 114°E (Figure 4). These transitional regions are described in detail from different points of view by Shah and Sempéré (submitted manuscript, 1997), *Goff et al.* [1997], Ma and Cochran (submitted manuscript, 1997), and *Cochran et al.* [this issue].

The SEIR between 100° and 104°E includes the full transition from an EPR-like axial high to a deep rift valley over the course of three segments (Figure 4a). This area is bounded to the west by the 100°E transform and to the east by the 104°20'E propagator. This gradual transition is associated with a gradient (2.5 m/km) in axial depth from ~ 2450 m near

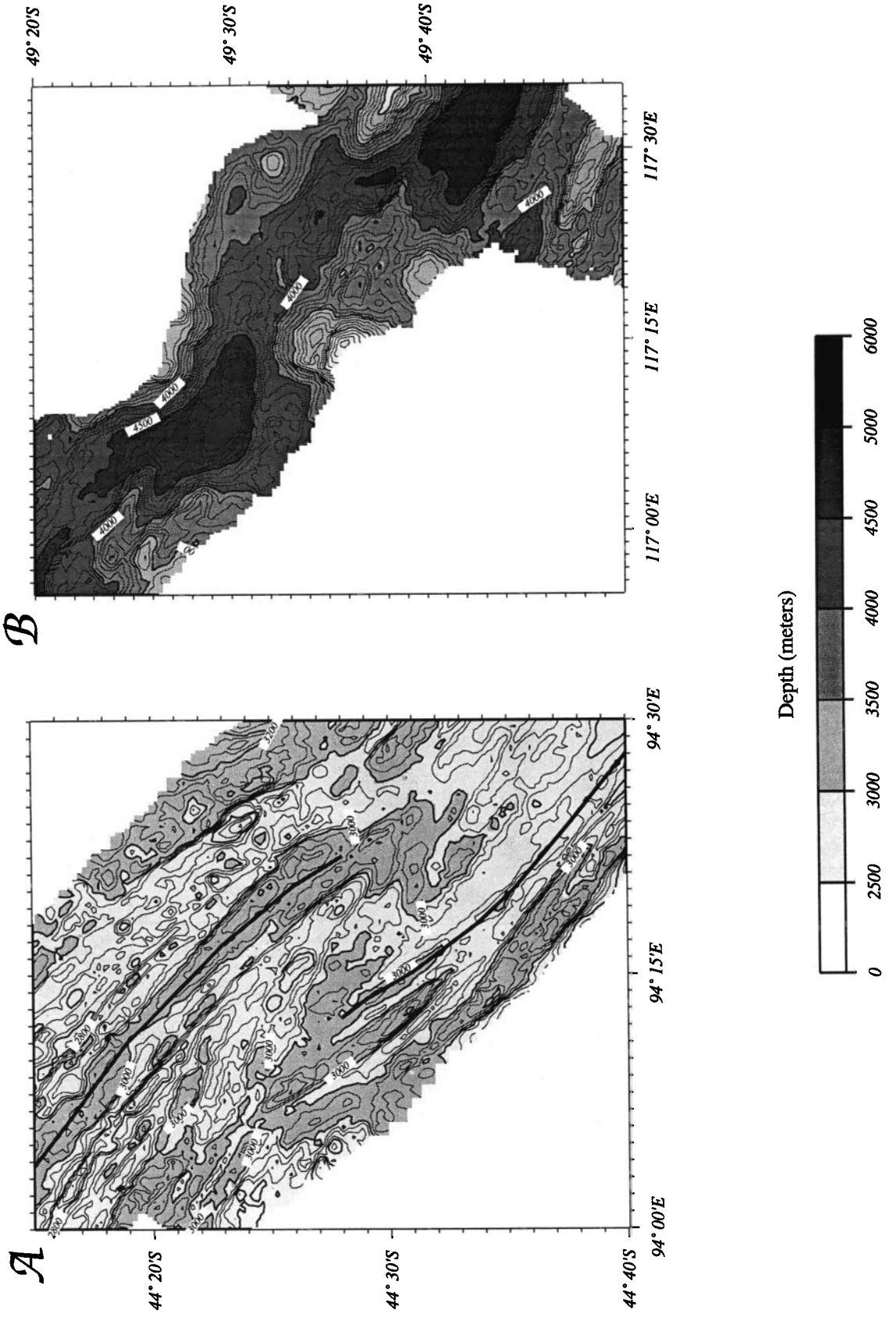

Figure 7. Morphology of nontransform offsets along the Southeast Indian Ridge. (a) Overlapping rifted highs near 94°15'E (contour interval is 50 m). This type of discontinuity accommodates small offsets along the SEIR predominantly west of 101°25'E, where the axial morphology is that of an axial high with faults developing more or less close to the axis. The location of the neovolcanic zone inferred from Seabeam data is shown as a solid line. (b) Nontransform discontinuity near 117°05'E and 117°25'E (contour interval is 100 m). Intrarift offsets such as are encountered along the slow spreading Mid-Atlantic Ridge (MAR) [*Grindlay et al.*, 1991; *Sempéré et al.*, 1993] are prevalent east of 101°25'E.

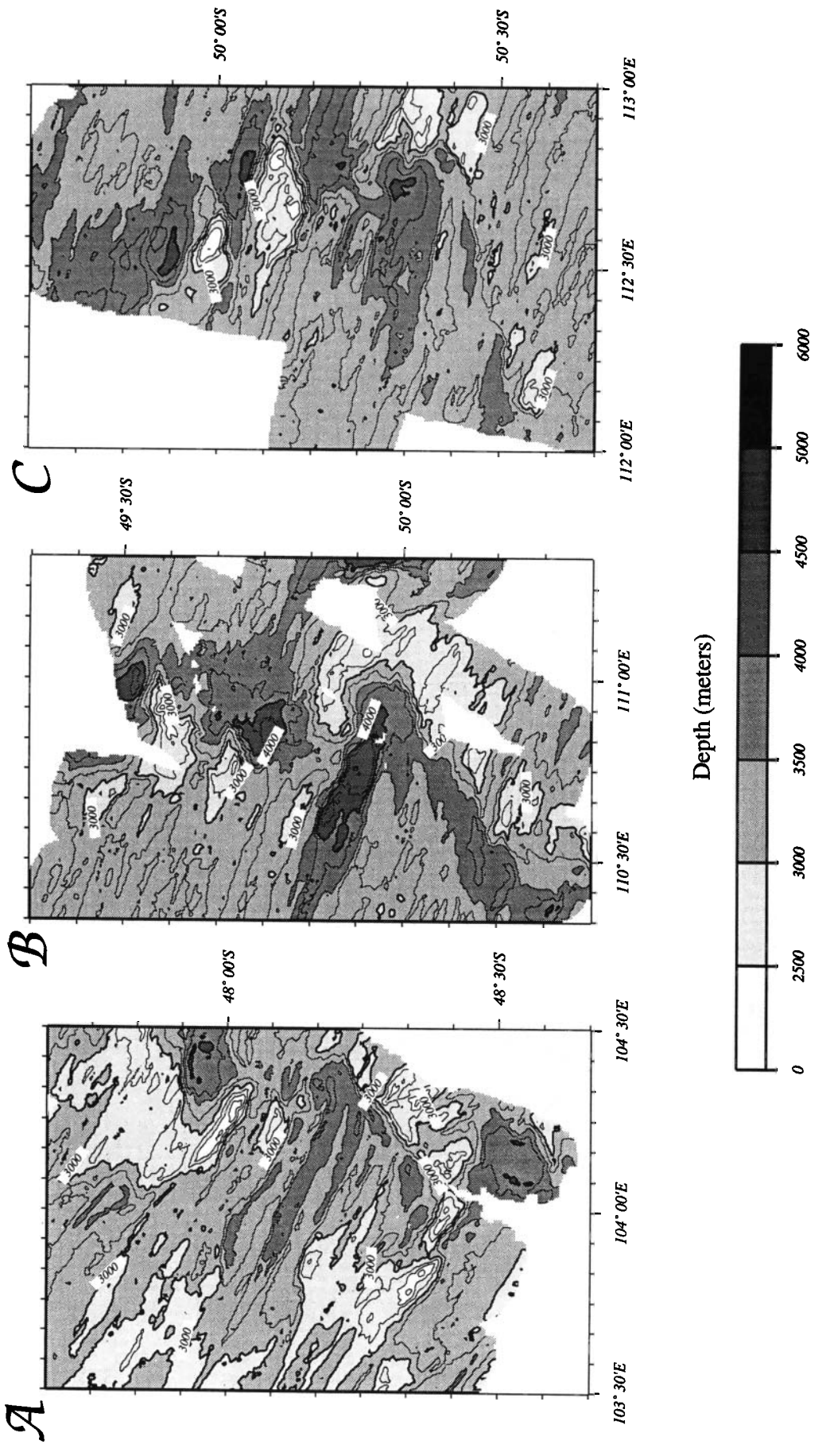

Figure 8. Examples of propagating rifts: (a) 104°20'E, (b) 111°00'E, (c) 112°45'E (contour interval is 250 m). These propagating rifts are migrating east toward the Australian-Antarctic Discordance at rates of 44, 31-37, and 53 mm yr^{-1}, respectively.

the middle of the western segment to 3950 m at the east end of the eastern segment. The evolution of morphology within this area is captured by profiles A, C, E, and I (Figure 6).

The two second-order segments located between 106° and 111°E each exhibit a progressive transition from a deep rift valley near the segment boundaries to a relative "high" near the middle of each segment (Figure 4b). Like the previous area, this region is bounded to the west by a transform (106°30'E) and to the east by a propagator (111°E). The two segments are separated by a complex fracture zone system. Axial depth increases westward within these two segments with a larger gradient of ~ 3.1 m/km. The axial high present in the western segment is located on top of a plateau bounded by outward facing faults parallel to the axis (profile B in Figure 6). This plateau gradually gives way to the east to a shallow axial valley (Figure 4b). The eastern segment is associated with a shallow rift valley which increases in depth and width toward the segment ends.

Between the 112°45'E propagating ridge and the 114°E transform, the spreading center is characterized by a shallow axial valley, except for a short distance near 113°38'E where an axial high is observed (Figure 4). The segment east of the 114°E transform exhibits a rift valley with more than 1000 m of relief (profile J in Figure 6).

The three areas described above form the transitional zone on the basis of a stochastic analysis of abyssal hills on the flanks of the SEIR [*Goff et al.*, 1997]. Within this zone transitional between axial high and rift valley morphologies, the rms height and characteristic width and length of abyssal hills span large fractions of the global variation observed in the ocean basins (60, 33, and 85%, respectively). Thus the transition in axial morphology observed along the SEIR at constant spreading rate has a strong effect on the character of abyssal hills [*Goff et al.*, 1997].

Discussion

Variations in Axial Depth and Mantle Temperature Along the SEIR

The depth of the SEIR increases by 2100 m from 88°E to 118°E. Although this increase in depth toward the AAD is large, an even steeper regional slope is present along the Southeast Indian Ridge east of the AAD [*Sempéré et al.*, 1996]. Tomographic studies indicate an increase in seismic velocity from 88°E toward the AAD [*Roult et al.*, 1994; *Su et al.*, 1994]. Detailed studies of the AAD using Rayleigh waves [*Forsyth et al.*, 1987] and *S-SS* differential travel time [*Kuo*, 1993] confirm that the AAD is a cold region of the upper mantle. The temperature gradient inferred from seismic data and the depth increase of the spreading center toward the AAD from the east and west are likely to be due to both the pattern of convective mantle upwelling prevalent in the region and associated variations in mantle temperature and the change in morphology from an axial high to a rift valley. The cooling of the mantle toward the AAD will be associated with a decrease in crustal production and the formation of a deep rift valley. Upwelling of the deep mantle is occurring beneath the Amsterdam and Kerguelen hot spots. In contrast, the AAD has been postulated to be a sink for along-axis flow because it is easier to accommodate lithospheric separation by lateral migration of mantle along the ridge axis rather than upwelling of the subjacent mantle which is anomalously cold and viscous, as well as potentially downwelling [*Weissel and Hayes*, 1974; *Forsyth et al.*, 1987; *West et al.*, 1994, 1997]. The depth gradients on either side of the AAD may be due to regional, along-axis mantle flow beneath the SEIR toward the Discordance [*West et al.*, 1997]. Thus in addition to changes in the morphology of the ridge axis, the increase in depth along the Southeast Indian Ridge may be due to a combination of two mechanisms: (1) dynamic topography associated with convective upwelling east and west of the AAD and with along-axis flow of warm mantle toward the AAD, and (2) crustal thickness variations due to variations in the melt production rate with thinner crust toward the AAD. In the following sections, we discuss the relative contribution of these two mechanisms to the long-wavelength characteristics of the SEIR.

Models of mantle circulation due to density anomalies calculated from tomographic results predict a dynamic topography that is small relative to the observed depth increase in the study area (e.g., ~ 400 m from *Cazenave and Thoraval* [1994]). Although such calculations of dynamic topography are not well constrained at the wavelength of the study area, it is likely that variations in crustal thickness within our survey area are responsible for a large part of the observed depth increase. Downward continuation of the mantle Bouguer anomaly to a depth of 6 km beneath the seafloor provides an upper estimate for the magnitude of crustal thickness variations along the plate boundary. This is an upper bound because we assume that the Bouguer anomaly is solely due to crustal thickness variations which may not be the case especially beneath axial highs. The calculated crustal thickness has a mean value of ~ 7-8 km between 88° and 90°E and decreases steadily by ~ 2 km toward the east until 115°E (Figure 9). A rift valley characterizes the SEIR east of 115°E until the eastern boundary of the AAD. Our calculations indicate another ~ 2 km in crustal thinning between 115°E and 118°E. Most of this supplemental thinning occurs east of 116°E where we lack off axis coverage. Near the east end of the survey area, we calculate a crustal thickness of ~ 4 km. Although this estimate is low, it is not unreasonable since a crustal thickness of 4.2 km has been measured in the AAD near 127°E [*Tolstoy et al.*, 1995], confirming the estimate obtained from satellite gravity data [*West et al.*, 1994]. Thus the long-wavelength decrease in crustal thickness calculated from gravity data has an upper bound of ~ 4 km.

We can estimate the variations in mantle temperature which are consistent with the long-wavelength geophysical characteristics of the Southeast Indian Ridge using the model of *Klein and Langmuir* [1987] who have proposed a relationship between crustal thickness, axial depth and the initial and final pressures of melting. Using this relationship and assuming that the final pressure of melting is the same over the survey area and that the compensation depth is 200 km, the decrease in calculated crustal thickness is equivalent to a temperature decrease of ~ 80°C from west to east (~ 55°C if the final pressure of melting beneath the west side of the area is 2 kbar lower than beneath the east side). The Klein and Langmuir model yields a crustal thickness of ~ 3 km at the east end of our survey area. Using the numerical model of mantle upwelling and melting of *West et al.* [1994], we estimate the temperature variation between the ends of our survey area consistent with the decrease in our calculated crustal thickness at ~ 60°C. We conclude that the long-wavelength variations in the geophysical characteristics of the SEIR between 88°E and

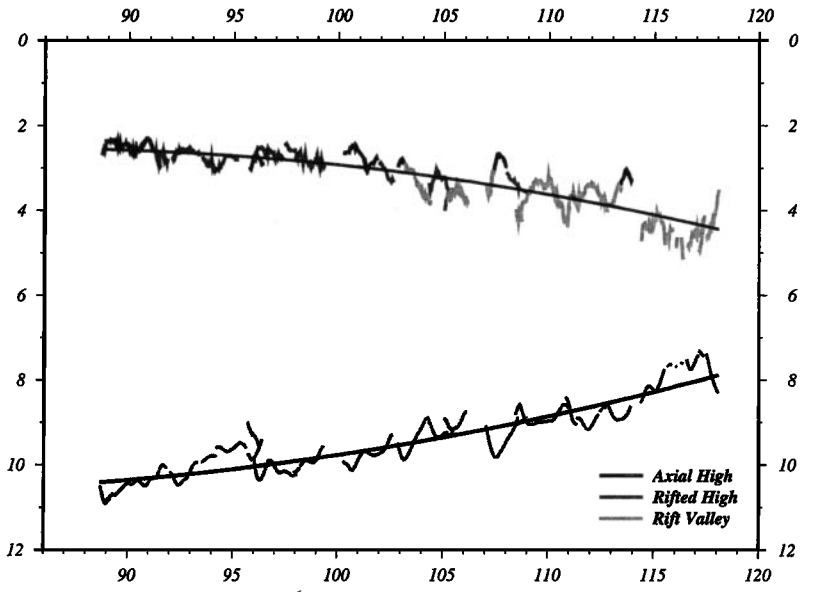

Figure 9. Calculated crustal thickness by downward continuation of Bouguer gravity anomalies along the plate boundary (bottom curve). Crustal thickness values have been smoothed by a Gaussian filter with a width of 75 km. The gravity data are consistent with a maximum decrease in crustal thickness of 4.5 km from east to west. Along-axis depth variations are coded by shading to indicate the type of axial morphology (top curve). The bold lines represent quadratic fits to the depth and crustal thickness variations.

118°E are consistent with a decrease in the subridge mantle temperature and in the melt production rate toward the AAD. This westward decrease in mantle temperature forms the basis of our proposed model schematically shown in Figure 10. Refinement of the estimate of temperature variation along the SEIR between 88°E and 118°E can be obtained by detailed analyses of ridge flank depth and gravity (Shah and Sempéré, submitted manuscript, 1997).

Examination of $Na_{8.0}$ from dredge samples shows that although basalts from the east end of the survey area are in agreement with the global array of Klein and Langmuir, samples from the west end are significantly more sodic than the global array [*Christie et al.*, 1995]. Using the Klein and Langmuir relationship and the segment average of $Na_{8.0}$ from our study area [*Christie et al.*, 1995], we obtain an equivalent axial depth of 3400 m, instead of 2300 m, and an equivalent crustal thickness of ~ 6 km, instead of the estimated 8 km, for the west end of the survey area. Therefore the depth of the spreading axis is shallower than it should be by ~ 1100 m based on the prediction of Klein and Langmuir. Thus although the model of Klein and Langmuir may provide a simple and suitable framework with which to study the influence of mantle temperature variations on the long-wavelength geophysical characteristics of the Southeast Indian Ridge, the uniformity in the composition of the underlying mantle and the details of the global correlation remain to be evaluated. The reader is referred to the companion paper by *Christie et al.* [this issue] for an extensive discussion of chemical variability along the Southeast Indian Ridge.

Although the SEIR at the wavelength of our study increases in depth toward the east, this increase is not monotonic. This nonuniformity in the depth gradient and the systematic displacement of the shallowest depth to the west in the four corridors that we have identified between 88°E and 111°E suggest that local processes are superposed on the long-wavelength variations in mantle temperature discussed above. The four intermediate-wavelength units that exhibit a uniform depth increase may constitute distinct supersegments along the Southeast Indian Ridge (Figure 3). Analysis of bathymetry and gravity data within the survey boxes indicates that the flow and temperature field of the mantle may be modified near the large offsets that bound the corridors to the east. Such a modification may arise from the interaction of eastward, along-axis flow beneath the SEIR with the large-offset transforms which perturb the continuity of the spreading axis (West and Sempéré, submitted manuscript, 1997).

We have observed that the relief in axial depth along segments increases from west to east (Figure 5). We interpret this increase as the result of the development of along-axis variations in crustal thickness and in mantle density structure beneath spreading segments. Such an increase in the amplitude of crustal thickness and mantle density variations at the segment scale is likely to arise from a combination of two conditions: (1) upwelling of the mantle becomes more focused beneath the middle of segments, and (2) lower crustal material preferentially emplaced in the segment center must be cold enough to prevent flow in response to horizontal pressure gradients [*Bell and Buck*, 1992; *Phipps Morgan* and *Chen*, 1993]. Focused mantle upwelling may result from the development of large viscosity contrast in the subridge mantle near the AAD [*Rabinowicz et al.*, 1993].

Transitions in Axial Morphology

The spreading rate variation present in the study area represents only ~ 4% of the global range. Spreading rate is therefore unlikely to exert alone a strong control on the long-wavelength changes in the geophysical characteristics of the plate boundary between 88°E and 118°E. Despite a uniform, intermediate spreading rate, the Southeast Indian Ridge reproduces variations in axial morphology and segmentation observed between spreading rates of ~0 and 120 mm yr^{-1} elsewhere.

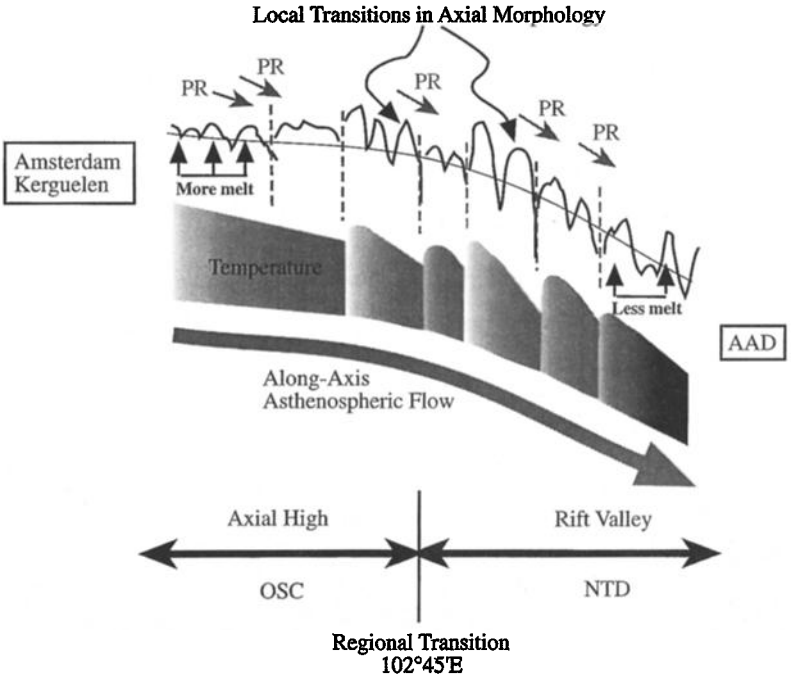

Figure 10. Sketch of proposed model of the Southeast Indian Ridge. In this model, the regional decrease in the depth of the spreading center is due to the decrease in the temperature of the subridge mantle (see gray shade) from 88°E to the Australian-Antarctic Discordance. Eastward along-axis flow of the asthenosphere may be associated with this decrease. The decrease in mantle temperature and the increase in axial depth are not uniform along axis. Propagating rifts (PR) along the SEIR between 88°E and 118°E are migrating eastward down the regional depth gradient and in the proposed direction of along-axis asthenospheric flow. The regional transition in the morphology of the axis and of the discontinuities that offset it is controlled by variations in the rheological structure of the axial lithosphere due to variations in the temperature of the mantle and in the related variations in the production of melt with respect to spreading rate. OSC: overlapping spreading centers; NTD: nontransform discontinuity.

Current models for the generation of axial topography invoke a threshold mechanism, based on variations in the thermal structure and rheological properties of oceanic crust and upper mantle, to account for the presence of axial highs or rift valleys [e.g., *Small and Sandwell*, 1989; *Chen and Morgan*, 1990a, b; *Phipps Morgan and Chen*, 1993]. Small variations in crustal thickness about a critical value for a given spreading rate may be related to transitions in axial topography. If these models are correct, the general evolution of the morphology of the SEIR from an axial high to the west to a rift valley to the east is consistent with the postulated decrease in the thickness of oceanic crust toward the AAD and the gradient in mantle temperature discussed previously. The transitions in axial morphology and the variations in calculated crustal thickness along the SEIR between 88°E and 118°E are in agreement with a ~ 6.0 km threshold in crustal thickness. This range of value is greater than the critical threshold in crustal thickness derived by *Phipps Morgan and Chen* [1993] (~4 km depending on the vigor of hydrothermal circulation) for the half spreading rate of the Southeast Indian Ridge.

An abrupt transition in axial morphology also occurs along the Southeast Indian Ridge near the eastern boundary of the Australian-Antarctic Discordance and to the east [*Weissel and Hayes*, 1974; *Sempéré et al.*, 1991]. East of this transition the SEIR is associated with an axial high, whereas it exhibits a rift valley in the AAD. The transition in morphology, like the increase in the axial depth, is much more abrupt east of the AAD than west of it. This difference indicates that the cause of the increase in depth and the change in morphology is not symmetric with respect to the AAD.

The fact that axial highs similar to the East Pacific Rise (EPR) are seldom seen along the SEIR but that, instead, rifted highs are more common leads us to suggest that a quasi-steady state, axial magma chamber is not present along most of the length of the SEIR even at the west end of our survey area [*Cochran et al.*, 1995, this issue]. The lack of such a permanent structure may account for the development of faults close to the inferred location of the neovolcanic zone and the predominance of rifted high morphology east of 102°45'E [*Cochran et al.*, 1995, this issue].

Nontransform Offsets

The spectrum of nontransform offsets observed along the SEIR between 88°E and 118°E includes those observed along fast, intermediate and slow spreading centers. We observe near 101°25'E a transition in the morphology of second-order discontinuities which is nearly coincident with the regional transition in axial morphology. Overlapping spreading centers (OSC) such as those observed along the East Pacific Rise (EPR) or the Juan de Fuca Ridge [*Macdonald et al.*, 1984] dominate west of 101°25'E, whereas discontinuities such as those observed on the Mid-Atlantic Ridge (MAR) [*Grindlay et*

al., 1991; *Sempéré et al.*, 1990] are prevalent east of 101°25'E. The geometry of overlapping spreading centers (OSC) suggests that the thermal structure at these offsets is such that the offset limbs of the spreading center behave as cracks in the lithosphere [*Pollard and Aydin*, 1984; *Sempéré and Macdonald*, 1986]. In contrast, the morphology of nontransform offsets such as are observed along slow spreading centers is indicative of a stronger lithosphere and thus a cooler thermal regime [*Grindlay et al.*, 1991]. Thus the presence of a transition in the morphology of discontinuities is consistent with our other observations.

Conclusions

We have studied the geophysical characteristics of the Southeast Indian Ridge between 88°N and 118°E. Our study supports the following conclusions:

1. The depth of the Southeast Indian Ridge increases by 2100 m from 88°E to 118°E. This long-wavelength increase is correlated with an increase in shear wave velocity and corresponds to a regional evolution from axial high topography to the west to rift valley topography to the east. The depth increase observed at the wavelength of the survey area is likely due to the general evolution from an axial high to a rift valley superposed on variations in crustal thickness resulting from variations in the temperature of the subridge mantle. Only a small contribution, if any, is expected from dynamic topography.

2. The Southeast Indian Ridge between 88°E and 118°E exhibits, at nearly constant spreading rate, the range in axial morphology displayed by the East Pacific Rise (EPR) and the Mid-Atlantic Ridge (MAR) and usually associated with variations in spreading rate. Although axial highs similar to the East Pacific Rise (EPR) are present, the typical axial high along the SEIR is characterized by a summit depression often encountered at intermediate rate ridges. The transitions in axial morphology observed along the SEIR may arise from a threshold mechanism.

3. The morphology of nontransform discontinuities (NTD) evolves from west to east from offsets typically encountered on fast and intermediate accreting plate boundaries to discontinuities present along slow spreading centers. This evolution is consistent with a strengthening of the axial lithosphere from west to east.

4. The long-wavelength changes observed along the Southeast Indian Ridge can be attributed to an inferred gradient in mantle temperature between regions influenced by the Amsterdam and Kerguelen hot spots and the Australian-Antarctic Discordance. However, local processes, perhaps associated with an heterogeneous mantle or along-axis asthenospheric flow perturb crustal accretion beneath this spreading center, giving rise to local transitions in axial topography and depth anomalies.

5. Although spreading rate is likely to exert the most important control of crustal accretion along the global mid-ocean ridge system, extreme variations in mantle temperature and melt production rate can reproduce the variability in crustal accretion due to variations in spreading rate. The transition in axial morphology along the SEIR is not abrupt. Instead, it occurs gradually through a series of local morphological transitions. Thus local conditions in mantle upwelling and the thermal structure of the axial lithosphere are important. In particular, modification to mantle upwelling may arise due to along-axis flow.

Acknowledgments. We would like to thank Captain E. Buck and the crew of the R/V *Melville* of Scripps Institution of Oceanography for their assistance during the field program. We are also indebted to S. Smith, U. Albright, T. Porteus, J. Skinner, E. Heckman, and J. Charters for their help in acquiring and processing the geophysical data collected during legs WEST09MV and WEST10MV. We benefited from discussions with A. Briais, P. Lecroart, M. Monnereau, M. Rabinowicz, S. Rouzo, and C. Thoraval. We thank J. Karsten and G. Neumann for critically reviewing this manuscript. This paper was written while the lead author was on leave at the Groupe de Recherche en Géodésie Spatiale in Toulouse. J.C.S. thanks J.-F. Minster, A. Cazenave, M. Rabinowicz, and A. Briais, who made this stay possible. GMT [*Wessel and Smith*, 1991] and the MB system software package of D. Caress and D. Chayes were used extensively throughout this study. This study was funded by the National Science Foundation (contracts OCE-9403583 to J.C.S. and OCE-9302091 to J.R.C.). LDEO contribution 5637.

References

Bell, R. E., and W. R. Buck, Crustal control of ridge segmentation inferred from observations of the Reykjanes Ridge, *Nature, 357*, 583-586, 1992.

Cazenave, A., and C. Thoraval, Mantle dynamics constrained by degree 6 surface topography, seismic topography and geoid: Inference on the origin of the South Pacific Superswell, *Earth Planet. Sci. Lett., 122*, 207-219, 1994.

Chen, Y., and W. J. Morgan, Rift valley/no rift valley transition at mid-ocean ridges, *J. Geophys. Res., 95*, 17,571-17,581, 1990a.

Chen, Y., and W. J. Morgan, A non-linear rheology model for mid-ocean ridge axis topography, *J. Geophys. Res., 95*, 17,583-17,604, 1990b.

Christie, D. M., B. Sylvander, and F. Sprtel, Major element variability of basalts from the Southeast Indian Ridge between 88°E and 118°E, *Eos Trans. AGU, 76 (46)*, Fall Meet. Suppl., F529, 1995.

Cochran, J. R., C. Small, Y. Ma, and J.-C. Sempéré, Modes of crustal accretion at intermediate spreading rates: The Southeast Indian Ridge between 88°E and 120°E, *Eos Trans. AGU, 76 (46)*, Fall Meet. Suppl., F529, 1995.

Cochran, J. R., J.-C. Sempéré, and SEIR Scientific Team, The Southeast Indian Ridge between 88°E and 118°E: Gravity anomalies and crustal accretion at intermediate spreading rates, *J. Geophys. Res.*, this issue.

DeMets, C., R. G. Gordon, D. F. Argus, and S. Stein, Current plate motions, *Geophys. J. Int. 101*, 425-478, 1990.

Forsyth, D. W., R. L. Ehrenbard, and S. Chapin, Anomalous upper mantle beneath the Australian-Antarctic Discordance, *Earth Planet. Sci. Lett., 84*, 471-478, 1987.

Goff, J. A. , Y. Ma, A. Shah, J. R. Cochran, and J.-C. Sempéré, Stochastic analysis of seafloor morphology on the flanks of the Southeast Indian Ridge: The influence of ridge morphology on the formation of abyssal hills, *J. Geophys. Res.*, in press, 1997.

Grindlay, N. R., P. J. Fox, and K. C. Macdonald, Second-order ridge axis discontinuities in the south Atlantic: Morphology, structure, and evolution, *Mar. Geophys. Res., 13*, 21-50, 1991.

Haymon, R. M., D. J. Fornari, M. H. Edwards, S. Carbotte, D. Wright, and K. C. Macdonald, Hydrothermal vent distribution along the East Pacific Rise crest (9°09'N, 9°54'N) and its relationship to magmatic and tectonic processes on fast-spreading mid-ocean ridges, *Earth Planet. Sci. Lett., 55*, 75-86, 1991.

Klein, E. M., and C. H. Langmuir, Global correlations of ocean ridge basalt chemistry with axial depth and crustal thickness, *J. Geophys. Res., 92*, 8089-8115, 1987.

Kuo, B.-Y., Thermal anomalies beneath the Australian-Antarctic Discordance, *Earth Planet. Sci. Lett., 119*, 349-364, 1993.

Lonsdale, P., Structural geomorphology of a fast-spreading rise crest: The East Pacific Rise near 3°25'S, *Mar. Geophys. Res., 3*, 251-293, 1977.

Ma, Y., and J. R. Cochran, Transitions in axial morphology along the Southeast Indian Ridge, *J. Geophys. Res., 101*,15,849-15,866, 1996.

Ma, Y., J. R. Cochran, C. Small, and J.-C. Sempéré, The Southeast Indian Ridge between 88°E and 120°E: Ridge flank morphology and abyssal hills, *Eos Trans. AGU, 76 (46)*, Fall Meet. Suppl., F529, 1995.

Macdonald, K. C., Mid-ocean ridges: Fine scale tectonic, volcanic, and hydrothermal processes within the plate boundary zone, *Annu. Rev. Earth Planet. Sci., 10*, 155-190, 1982.

Macdonald, K. C., and B. P. Luyendyk, Deep-tow studies of the

structure of the Mid-Atlantic Ridge crest near lat. 37°N, *Geol. Soc. Am. Bull.*, *88*, 621-636, 1977.

Macdonald, K. C., J.-C. Sempéré, and P. J. Fox, The East Pacific Rise from the Siqueiros to the Orozco fracture zone: Along strike continuity of the neovolcanic zone and the structure and evolution of overlapping spreading centers, *J. Geophys. Res.*, *89*, 6049-6069, 1984.

Neumann, G. A., and D. W. Forsyth, The paradox of the axial profile: Isostatic compensation along the axis of the Mid-Atlantic Ridge?, *J. Geophys. Res.*, *98*, 17891-17910, 1993.

Palmer, J., J.-C. Sempéré, D. Christie and J. Phipps Morgan, Morphology and tectonics of the Australian-Antarctic Discordance between 123°E and 128°E, *Mar. Geophys. Res.*, *15*, 121-152, 1993.

Phipps Morgan, J., and Y. J. Chen, The dependence of ridge-axis morphology and geochemistry on spreading rate and crustal thickness, *Nature*, *364* , 706-708, 1993.

Phipps Morgan, J., and D.T. Sandwell, Systematics of ridge propagation south of 30°S, *Earth Planet. Sci. Lett.*, *121*, 245-258, 1994.

Pollard, D. D., and A. Aydin, Propagation and linkage of oceanic ridge segments, *J. Geophys. Res.*, *89*, 10,017-10,028, 1984.

Rabinowicz, M., S. Rouzo, J.-C. Sempéré, and C. Rosemberg, Three-dimensional models of mantle flow beneath spreading centers, *J. Geophys. Res.*, 98, 7851-7870, 1993.

Roult, G., D. Rouland, and J.-P. Montagner, Antarctica II: Upper mantle structure from velocities and anisotropy, *Phys. Earth. Planet. Inter.*, *84*, 33-57, 1994.

Scheirer, D. S., and K. C. Macdonald, Variation in cross-sectional area of the axial ridge along the East Pacific Rise: Evidence for the magmatic budget of a fast spreading center, *J. Geophys. Res.*, *98*, 7871-7885, 1993.

Sempéré, J.-C., and K. C. Macdonald, Overlapping spreading centers: Implications from crack growth simulation by the displacement discontinuity method, *Tectonics*, *5*, 151-163, 1986.

Sempéré, J.-C., G. M. Purdy, and H. Schouten, The segmentation of the Mid-Atlantic Ridge between 24°N and 30°40'N, *Nature*, *344*, 427-431, 1990.

Sempéré, J.-C., J. Palmer, D. Christie, J. Phipps Morgan, and A. Shor, The Australian-Antarctic Discordance, *Geology*, *19*, 429-432, 1991.

Sempéré, J.-C., J. Lin, H. Brown, H. Schouten, and G. M. Purdy, Segmentation and Morphotectonic variations along a slow-spreading center: The Mid-Atlantic Ridge (24°00'N-30°40'N), *Mar. Geophys. Res.* , *15*, 153-200, 1993.

Sempéré, J.-C., C. Small., A. Shah, B. P. West, D. M. Christie, J. R. Cochran, and L. Géli, Long-wavelength variations in segmentation characteristics along the Southeast Indian Ridge between 88°E and 120°E: Influence of a mantle temperature gradient between Kerguelen/Amsterdam and the Australian-Antarctic Discordance (abstract), *Eos Trans. AGU, 76 (46)*, Fall Meet. Suppl., F529, 1995.

Sempéré, J.-C., B. P. West, and L. Géli, The Southeast Indian Ridge between 127° and 133°E: Contrasts in segmentation characteristics and implications for crustal accretion, in *Tectonic, Magmatic, Hydrothermal and Biological Segmentation of Mid-Ocean Ridge*, edited C. J. McLeod, P. A. Tyler and C. L. Walker, *Geol. Soc. Spec. Publ.*, *118*, 1-15, 1996.

Shah, A., J.-C. Sempéré, B. P. West, and J. R. Cochran, Transitions in morphology along the Southeast Indian Ridge between 100°E and 111°E: Constraints from tectonic studies, *Eos Trans. AGU*, *76* (46), Fall Meet. Suppl., F570, 1995.

Small, C., and D. T. Sandwell, An abrupt change in ridge axis gravity with spreading rate, *J. Geophys. Res.*, *94*, 17,383-17,392, 1989.

Small, C., and D. T. Sandwell, An analysis of ridge axis gravity roughness and spreading rate, *J. Geophys. Res.*, *97*, 3235-3245, 1992.

Small, C., J.-C. Sempéré, J. R. Cochran, and D. M. Christie, The segmentation of the Southeast Indian Ridge (88°E-120°E), *Eos Trans. AGU, 76* (46), Fall Meet. Suppl., F570, 1995.

Su, W.-J., R. L. Woodward, and A.M. Dziewonski, Degree 12 model of shear velocity heterogeneity in the mantle, *J. Geophys. Res.*, *99*, 6945-6980, 1994.

Tolstoy, M., A. J. Harding, J. A. Orcutt, and J. Phipps Morgan, A seismic refraction investigation of the Australian-Antarctic Discordance and neighboring South East Indian Ridges: Preliminary results, *Eos Trans. AGU, 76* (17), Spring Meet. Suppl., S275, 1995.

Vogt, P.R., N.K. Cherkis, and G.A. Morgan, Project Investigator, Evolution of the Australian-Antarctic Discordance from a detailed aeromagnetic study, in *Antarctic Earth Science: Proceedings of the 4th International Symposium on Antarctic Earth Sciences*, edited by R.L. Oliver, P.R. James, and J. Jago, pp. 608-613, Aust. Acad. of Sci., Canberra, 1984.

Weissel, J. K., and D. E. Hayes, The Australian-Antarctic Discordance: New results and implications, *J. Geophys. Res.*, *79*, 2579-2587, 1974.

Wessel, P., and W. H. F. Smith, Free software helps map and display data, *Eos Trans. AGU, 72*, 411, 445-446, 1991.

West, B. P., J.-C. Sempéré, D. G. Pyle, J. Phipps Morgan, and D. M. Christie, Evidence for variable upper mantle temperature and crustal thickness in and near the Australian-Antarctic Discordance, *Earth Planet. Sci. Lett.*, *128*, 135-153, 1994.

West, B. P., W. S. D. Wilcock, J.-C. Sempéré, and L. Géli, Three-dimensional structure of asthenospheric flow beneath the Southeast Indian Ridge, *J. Geophys. Res.*, *102*, 7,783-7,802, 1997.

Yan, B., K. Graham, and K. P. Furlong, Lateral variations in upper mantle thermal structure inferred from three-dimensional seismic inversion models, *Geophys. Res. Lett.*, *16*, 449-452, 1989.

D. Christie and B. Sylvander, College of Oceanic and Atmospheric Sciences, Orgeon State University, Corvallis, OR 97331-5503.

J. R. Cochran, Y. Ma, C. Small, and W. Zhang, Lamont-Doherty Earth Observatory of Columbia University, Palisades, NY 10964.

M. Eberle, Department of Geological Sciences, Brown University, Providence, RI 02912.

L. Géli, Département de Géosciences Marines, Institut Français de Recherche pour l'Exploitation de la Mer, B. P. 70, 29280 Plouzané, France.

J. A. Goff, University of Texas Institute of Geophysics, 8701 N. MoPac Expressway, Austin, TX 78759.

H. Kimura, Earthquake Research Institute , University of Tokyo, 1-1-1 Yayoi, Bunkto-ku, Tokyo, 113 Japan.

J.-C. Sempéré, Exxon Production Research Company, P. O. Box 2819, Houston, TX 77252-2189.

A. Shah and B. P. West, School of Oceanography, University of Washington, P. O. Box 357940, Seattle, WA 98195-7940.

(Received June 10, 1996; revised December 28, 1996;
accepted January 15, 1997.)